Applied Catalysis B: Environmental 152–153 (2014) 184–191

Contents lists available at ScienceDirect

Applied Catalysis B: Environmental

journal homepage: www.elsevier.com/locate/apcatb

Catalytic and adsorption studies for the hydrogenation of CO_2 to methane

C. Janke [1], M.S. Duyar, M. Hoskins, R. Farrauto *

Earth and Environmental Engineering Department, Columbia University in the City of New York, 500 West 120th Street, New York, NY 10027, United States

ARTICLE INFO

Article history:
Received 8 November 2013
Received in revised form 9 January 2014
Accepted 11 January 2014
Available online 27 January 2014

Keywords:
Ru/Al_2O_3 particles and monolith
CO_2 methanation
Thermal and cyclic stability
TGA/DSC adsorption studies
Carbon neutrality

ABSTRACT

CO_2 methanation has been evaluated as a means of storing intermittent renewable energy in the form of synthetic natural gas. A range of process parameters suitable for the target application (4720 h^{-1} to 84,000 h^{-1} and from 160 °C to 320 °C) have been investigated at 1 bar and $H_2/CO_2 = 4$ over a 10% Ru/γ-Al_2O_3 catalyst. Thermodynamic equilibrium was reached at T ≈ 280 °C at a GHSV of 4720 h^{-1}. Cyclic and thermal stability tests specific to a renewable energy storage application have also been conducted. The catalyst showed no sign of deactivation after 8 start-up/shut-down cycles (from 217 °C to RT) and for total time on stream of 72 h, respectively. In addition, TGA-DSC was employed to investigate adsorption of reactants and suggest implications on the mechanism of reaction. Cyclic TGA-DSC studies at 265 °C in CO_2 and H_2, being introduced consecutively, suggest a high degree of short term stability of the Ru catalyst, although it was found that CO_2 chemisorption and hydrogenation activity was lowered by a magnitude of 40% after the first cycle. Stable performance was achieved for the following 19 cycles. The CO_2 uptake after the first cycle was mostly restored when using a H_2-pre-treatment at 320 °C between each cycle, which indicated that the previous drop in performance was not linked to an irreversible form of deactivation (sintering, permanent poisoning, etc.). CO chemisorption on powder Ru/γ-Al_2O_3 was used to identify metal sintering as a mechanism of deactivation at temperatures higher than 320 °C. A 10% Ru/γ-Al_2O_3//monolith has been investigated as a model for the design of a catalytic heat exchanger. Excellent selectivity to methane and CO_2 conversions under low space-velocity conditions were achieved at low hydrogenation temperatures (T = 240 °C). The use of monoliths demonstrates the possibility for new reactor designs using wash-coated heat exchangers to manage the exotherm and prevent deactivation due to high temperatures.

1. Introduction

The efficient utilization of renewable energy resources from wind turbines and solar panels is still an ongoing challenge. Naturally, electrical power from wind and solar devices is intermittent and the energy is produced at locations where it is not directly consumed. Thus, solutions for long-range transportation and storage of renewable energies are currently of great interest [1–3]. Naturally occurring renewable energy sources can be utilized to generate H_2 by electrolysis of water. Carbon dioxide, captured from natural gas combustion and other sources, can be combined with H_2 and catalytically converted to synthetic natural gas (SNG) or methane. The CO_2 methanation reaction is shown below (Eq. (1)).

$$CO_2 + 4H_2 \leftrightarrow CH_4 + 2H_2O,\ \Delta H = -164\ kJ/mol \quad (1)$$

This process concept utilizes CO_2 as C1 building block to produce SNG as fuel. Consequently, the amount of imported natural gas for power generation is reduced, saving operating costs, while simultaneously reducing green-house gas emissions and avoiding waste of renewable energy [4]. In the light of this potential application, this study revisits the direct hydrogenation of carbon dioxide.

Note that the CO_2 hydrogenation is strongly exothermic and thermodynamically favored at low temperatures, where kinetic rates are low. Thus, heat management is crucial to avoid catalyst damage and to utilize the released heat effectively. Managing heat in a fixed bed reactor can be difficult due to the tendency of hot spot formation. Both endothermic and exothermic heat transfer issues can be avoided by depositing the hydrogenation catalyst on a heat exchanger as it has been shown successfully e.g. for natural gas steam reforming [5]. To implement such technology, a highly active hydrogenation catalyst is needed for two reasons. First of all, the amount of wash-coat on a heat exchanger is limited to a thin layer no more than about 200 μ. Secondly, according to the thermodynamic equilibrium, the catalyst is required to show high activity below 350 °C in order to maximize the yield of methane

* Corresponding author. Tel.: +1 212 854 6390; fax: +1 732 438 1090.
E-mail address: rf2182@Columbia.edu (R. Farrauto).
[1] BASF, Carl-Bosch Strasse 38, D-67056 Ludwigshafen, Germany.

0926-3373/$ – see front matter © 2014 Elsevier B.V. All rights reserved.
http://dx.doi.org/10.1016/j.apcatb.2014.01.016

at 1 bar and at a stoichiometric H_2/CO_2 ratio of 4. At temperatures higher than 350 °C, steam reforming of methane becomes thermodynamically favorable resulting in limited amounts of methane and an increase in CO and CO_2. In addition to a high catalyst activity, the catalyst must be resistant against deactivation caused by sintering or/and carbon deposition and must survive start-up/shut-down cycles with various time-on-stream (TOS). The start/stop requirement is based on intermittent solar or wind available to produce the H_2.

In the last three decades, studies of CO_2 methanation have intensively focused on various supported catalysts. Catalysts based on Ni [6,7], Ru [8], Rh [9–11], Pd [12–14], Fe[15] or Co [16,17] have been identified. Carrier or supports such as Al_2O_3 [18], SiO_2 [19], ZrO_2 [20], CeO_2 [21], La_2O_3 [22], MgO [23], TiO_2 [24], carbon materials [25] and zeolites [26] have been used to support the active metals. Doping and promoting effects have been evaluated as well [27–29]. Among these catalytic systems, a Ru-based catalyst seems to be a good choice when supported on the inexpensive carrier γ-Al_2O_3 [30–32] due to its high activity per gram and is thus suitable for wash-coating technology.

The motivation behind the current work is to search for carbon neutral sources of power, utilizing captured CO_2 and renewable "green H_2" (from wind, solar etc.). The CO_2 generated from a facility that combusts CH_4 (e.g. natural gas) for power, is to be captured and catalytically combined with "green H_2" to produce synthetic natural gas. This reduces CO_2 emissions, utilizes H_2 from electrolysis and recycles the methane, decreasing the need for new natural gas.

In this work, the catalytic properties of Ru/γ-Al_2O_3 have been probed as a function of process parameters and cyclic stability towards start-up/shut-down cycles in a traditional fixed bed reactor. TGA-DSC studies in CO_2 and H_2-containing feeds have been performed to evaluate further catalytic stability and mechanistic insights. To further probe the catalytic properties of Ru/γ-Al_2O_3 wash-coat on a monolith, a 10% Ru/γ-Al_2O_3//monolith was also investigated, used as model system for a wash-coated heat exchanger.

2. Experimental

2.1. Catalyst

The Ru/γ-Al_2O_3 was supplied by BASF and was synthesized by incipient wetness impregnation of γ-Al_2O_3 with a nitrate salt of ruthenium. The Ru-loading was adjusted to 10 wt.%. The impregnated powder was dried at 120 °C and calcined in air at 250 °C for 2 h to decompose the precursor salt. The calcination temperature of 250 °C was chosen to prevent the formation of volatile ruthenium oxides which become favorable at higher temperatures. The catalyst was used as received for the catalytic tests and reduced in situ in the process gas (see below for composition). The internal surface area of the fresh catalyst was determined with the single-point BET surface area method at 77 K using the ChemBET Pulsar TPR/TPD unit (Quantachrome). Three measurements were made for each sample. The average surface area was found to be 51 m^2/g.

A cordierite monolith was wash-coated with an aqueous slurry containing 10% Ru/γ-Al_2O_3. It was dried at 120 °C and calcined at 200 °C in air for 8 h. The loading was 2 g/in^3. The wash-coated monolith has been used for catalytic tests as received and was also reduced in situ in the process gas.

2.2. Catalytic tests

Catalytic tests were performed in a fixed bed glass reactor with an inner diameter of 12 mm at 1 bar. The catalyst was pressed to pellets and crushed and sieved to obtain a particle fraction of 610–700 μm in diameter. The reactor was loaded with 1 volume catalyst to 1.25 volumes of quartz. The space velocity GHSV, was varied from 4720 h^{-1} to 84,000 h^{-1}. The temperature at the exit of catalyst bed was measured and is defined in this work as hydrogenation reaction temperature. The temperature of the furnace was controlled by an additional thermocouple, placed at the inlet of the catalyst bed. A reaction mixture of 4 vol.% CO_2, 16 vol.% H_2 ($4H_2/1CO_2$) with the balance He was used. The flow was controlled by a rotameter. Water was condensed at the exit to allow measurement of product gases (CH_4, CO, CO_2, and H_2). The water level in the cold trap was low enough to prevent absorption of any gases. The reaction mixture was heated to the desired inlet temperature varied from 160 °C to 320 °C. A blank test with only quartz beads showed no conversion of H_2 or CO_2. Analysis of the product distribution was performed on-line with a micro GC (GC 3000 A, Inficon) equipped with a Molsieve column to measure H_2, He, CH_4 and CO concentrations. A Plot U column was used to detect CO_2. An OV-1 column and alumina column was used to monitor the formation of light hydrocarbons and olefins. Neither olefins nor $C1^+$ hydrocarbons were detected under any reaction conditions. Helium was used as internal standard. Results in this work are given in vol.% on a dry basis including the He concentration.

Catalytic tests using a fixed bed reactor and Ru/γ-Al_2O_3//monolith were performed under identical conditions. The gaseous space velocity GHSV of the monolith was calculated based on the total volume occupied by the monolith. The volumetric space velocity was set to 108 h^{-1}. The weight hourly space velocity WHSV was 0.9 L h^{-1} g^{-1} at a wash-coat loading of 2 g/in^3. Carbon balances were calculated for each test and were repeatedly between 99 and 101%.

The Ru/γ-Al_2O_3 particulate catalyst was exposed to eight start-up/shut-down cycles having different reaction times, ranging from 1 to 24 h at 217 °C and GHSV = 4720 h^{-1}. A fresh sample of Ru/γ-Al_2O_3 was first heated in the H_2/CO_2/He mixture to the reaction temperature and then kept under these conditions. The system was cooled to room temperature in Ar, followed by reheating in the H_2/CO_2/He stream to 217 °C.

2.3. Cyclic TGA-DSC studies

The cyclic temperature-programmed-oxidation-reduction study, a combination of alternating TPO and TPR cycles and the cyclic stability tests in CO_2 and H_2 were performed with fresh Ru/γ-Al_2O_3 particulate powder in a Jupiter STA 449 F3 instrument (Netsch). Typically, 50 mg of the catalyst powder was placed into an alumina crucible and a blank test was performed prior to the measurement with an empty cell under the experimental reaction condition. The sensitivity calibration for the DSC mode was performed in a flow of N_2 using In, Sn, Bi, Zn and Al as the calibration standard.

For the cyclic TPR/TPO study, the fresh sample was exposed first to 2% H_2/N_2 and the temperature was raised with a ramp of 5 K/min to 320 °C (TPR). After cooling in N_2 to room temperature the catalyst was exposed to 1% O_2/N_2 and the temperature was raised to 320 °C (TPO) with 5 K/min. The TPO and TPR tests were applied consecutively 3 times each (6 cycles in total) to the catalyst to obtain information about the redox-properties and indirectly the sintering behavior of the catalyst.

The cyclic hydrogenation test in CO_2/N_2 and H_2/N_2 was performed isothermally. After reducing the sample at 320 °C in 2% H_2/N_2, the catalyst was exposed initially to 0.5% CO_2/N_2 at 260 °C for 90 min, followed by a purge in pure N_2 for 30 min and finally to 2% H_2/N_2 for 90 min. One full hydrogenation cycle consists of CO_2 adsorption and subsequent H_2 treatment with a N_2 purge in-between. 20 cycles were conducted consecutively. The weight loss

and gain in the thermogram and the exothermic signals in the heat flux function from the DSC mode were used as an indication of hydrogenation activity. The WHSV in this cyclic test was 14.4 L h^{-1} g^{-1}. For comparison catalytic activity in the fixed bed reactor over Ru/γ-Al_2O_3 particulates, the highest space-velocity (84,000 h^{-1}) corresponds to a WHSV of 88.6 L h^{-1} g^{-1} and the lowest (4720 h^{-1}) to a WHSV of 5.1 L h^{-1} g^{-1}.

In addition, regeneration in-between each hydrogenation cycle was performed at 320 °C with 2% H_2/N_2. The CO_2 uptake capacity for each cycle relative to the capacity in the first cycle was calculated to judge the success of the H_2 pre-treatment. It was derived from:Relative CO_2uptake capacity $= \left(\frac{\Delta w_n}{\Delta w_1}\right) \times 100\%$where Δw_n is the weight gain during CO_2 introduction in cycle n and Δw_1 is the weight gain during CO_2 introduction in the first cycle. Weight gains observed during CO_2 introduction periods were assumed to be associated only with the chemisorption of CO_2 on the catalyst.

2.4. Metal dispersion by CO chemisorption

CO chemisorption was performed using a ChemBET Pulsar TPR/TPD unit (Quantachrome). The fresh Ru/γ-Al_2O_3 sample was placed inside the U shaped sample holder of the ChemBET Pulsar TPR/TPD unit and degassed to remove any vapors in the sample. Subsequently, the sample was reduced in situ, in 4% H_2/N_2 (60 mL/min) at a temperature of either 250, 320, 350, or 550 °C for 1 h. Following reduction, the sample was brought to room temperature in helium. CO (100% purity) chemisorption of pretreated samples was performed at RT.

3. Results and discussion

3.1. Catalytic tests over Ru/γ-Al_2O_3 particles

3.1.1. Impact of reaction temperature and space velocity

The catalytic performance as a function of the reaction temperature and GSHV is shown in Fig. 1. The equilibrium composition is shown as the red (solid line w/o data points) line for CO_2, CH_4 and CO.

It is clear that the space velocity and reaction temperature impact the product distribution significantly. At GHSV = 4720 h^{-1} the thermodynamic equilibrium is almost reached at 280 °C. However, increased GHSV results in lower CO_2 conversion with some CO formation. The increase in CO formation with increasing space velocity is accompanied by a decrease in CO_2 conversion and a shift of the maximum activity to higher reaction temperatures. In principle, CO formation can occur mostly by the reversed water gas shift reaction (RWGS)(Eq. (2)) with a small contribution depending on temperature from steam reforming (SR) of methane (Eq. (3)).

$$CO_2 + H_2 \rightarrow CO + H_2O \quad (2)$$

$$CH_4 + H_2O \rightarrow CO + 3H_2 \quad (3)$$

In several publications it was reported that for CO and CO_2 containing feed mixtures, CO hydrogenation occurs at lower temperatures over supported Ru-containing catalysts [33–35]. For instance, it has been shown that the CO methanation is favored kinetically over that of CO_2 below 300 °C for 0.5% Ru/Al_2O_3, even when the CO_2 concentration was 15 times higher than the CO at CO_2/H_2 = 3.3 [34]. Considering these results, CO formation as a by-product is initially surprising. However, in agreement with our results, it has been also shown in this work [34] that with increasing temperature and increasing space velocity CO conversion to CH_4 decreases significantly relative to CO_2 conversion. The authors also attributed this to an increasing contribution from the RWGS reaction. Accordingly, the rate of the reverse water gas shift reaction is much faster than the rate of CO hydrogenation. In addition, it has been suggested in several publications that CO_2 hydrogenation is initiated by a dissociative adsorption of CO_2 (Eq. (4)) to CO and O, followed by dissociation of the latter species to C and O (Eq. (5)) and successive hydrogenation of C to CH_4 [36,37]. Other authors have proposed the formation of a formate intermediate at the metal-support interface, which decomposes to CO (Eq. (6)) and subsequently reacts with adsorbed hydrogen to form CH_4 [38,39]. Hence CO is also an intermediate in the CO_2 hydrogenation reaction.

$$CO_2(ads) \rightarrow CO(ads) + O(ads) \quad (4)$$

$$CO(ads) \rightarrow C(ads) + O(ads) \quad (5)$$

$$HCOO^-(ads) + H^+(ads) \rightarrow CO(ads) + H_2O(ads) \quad (6)$$

3.1.2. Impact of start-up/shut down cycles

To probe the stability of the Ru/γ-Al_2O_3 against start-up/shut-down cycles, a fresh sample was exposed to eight hydrogenation cycles at 4720 h^{-1} and T = 217 °C. Each of these cycles differed in its length. The shortest cycle had a duration of 1 h and the longest a duration of 20 h. The total time on stream was 72 h. The CO_2, CH_4 and CO concentrations are plotted in Fig. 2 as a function of cycle

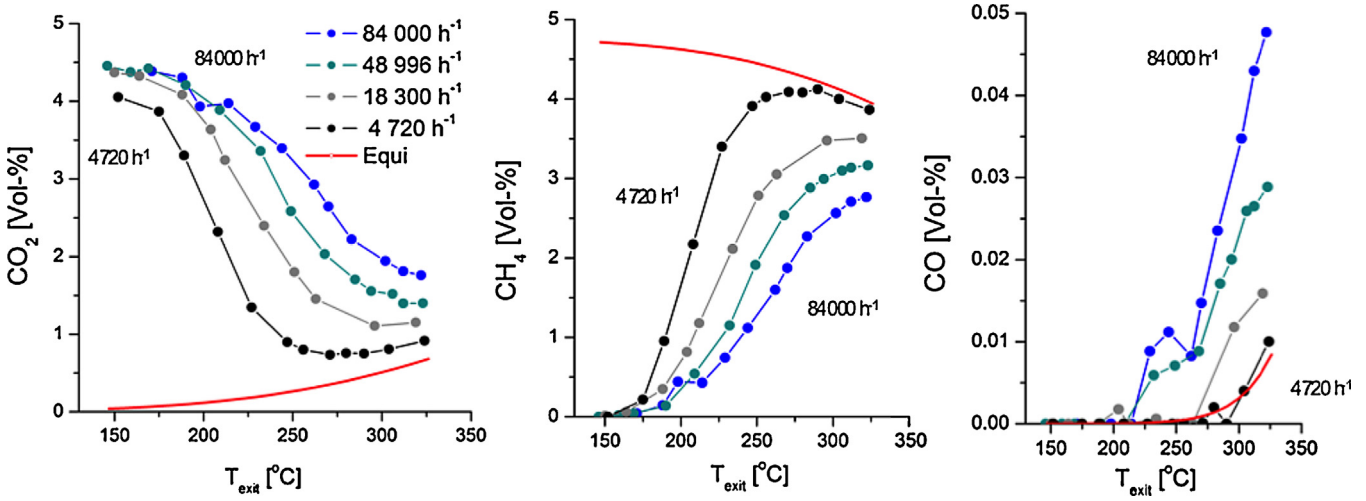

Fig. 1. Catalytic performance for Ru/γ-Al_2O_3 particles in a fixed bed reactor as a function of the reaction temperature for different GHSV at 1 bar and H_2/CO_2 = 4 (H_2:CO_2:He = 16:4:80 (in vol.%), left plot: CO_2 concentration, middle plot: CH_4 concentration, right plot: CO concentration, solid line with no data points: dry equilibrium concentrations.

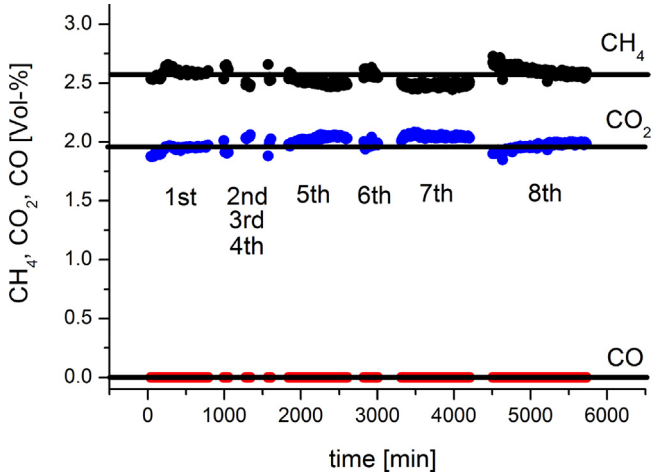

Fig. 2. Catalytic performance for Ru/γ-Al_2O_3 particles in a fixed bed reactor at GHSV = 4720 h^{-1}, T = 217 °C, p = 1 bar and H_2/CO_2 = 4 (H_2:CO_2:He = 16:4:80 (in vol.%) for eight start-up/shut-down cycles and 72 h TOS in total.

number and time, respectively. From this plot it is seen, that the catalyst does not deactivate and catalytic performance is recovered within each of the seven start-up cycles. Also CO was not detected in the stream after 72 h, thus methane selectivity is retained.

3.1.3. *Thermodynamic equilibria of the CO_2 hydrogenation reaction at atmospheric pressure*

As stated earlier the hydrogenation of CO_2 is highly exothermic (see ΔH in Eq. (1)). Fig. 3 displays the equilibrium distribution as a function of temperature at atmospheric pressure including H_2O, CH_4, CO_2, CO and C species. At higher temperatures, thermodynamic equilibrium favors steam reforming of methane and reverse water gas shift, both of which are endothermic processes. Hence both conversion and selectivity to methane decrease at temperatures greater than 350 °C. Exposure of the catalyst to high temperatures is also expected to result in deactivation due to sintering. Aging studies investigating such effects are also in progress. From the equilibrium product distribution shown in Fig. 3 it can be seen that a good heat management strategy can play a critical role in increasing conversions to methane as well as maintaining 100% selectivity. Efficient heat removal can be achieved by designing a methanation reactor in which the catalyst is washcoated onto

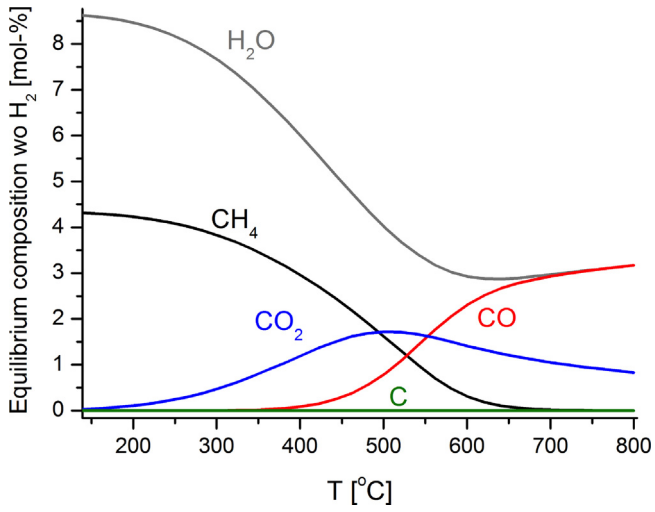

Fig. 3. Equilibrium distribution at atmospheric pressure as a function of temperature, including water and amorphous carbon species.

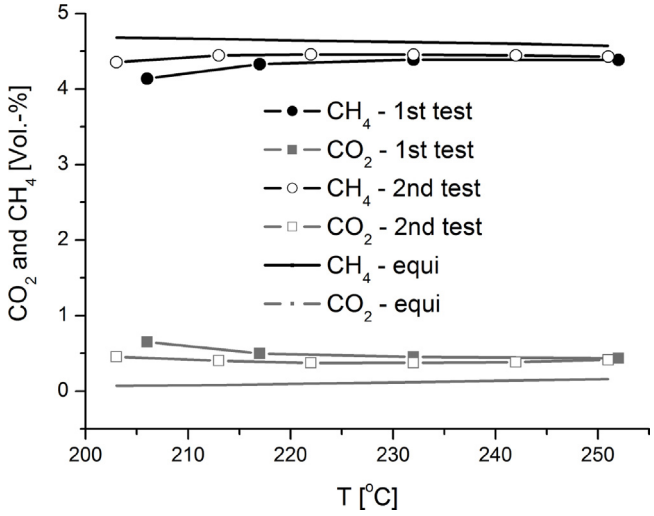

Fig. 4. Catalytic performance for CO_2 hydrogenation as a function of temperature over Ru/γ-Al_2O_3//monolith at GHSV = 108 h^{-1}, WHSV = 0.9 l/g h, p = 1 bar and H_2/CO_2 = 4 (H_2:CO_2:He = 16:4:80 (in vol.%), 1st test: fresh monolith, 2nd test: spent monolith.

a heat exchanger. The performance of the washcoated Ru/γ-Al_2O_3 catalyst (on a honeycomb monolith) as a model for such a system is discussed in the next section.

3.2. *Catalytic performance of Ru/γ-Al_2O_3//monolith*

A ceramic monolith (400 cpsi) wash-coated with Ru/γ-Al_2O_3 was tested. In Fig. 4, the equilibrium concentrations for CH_4 and CO_2 are compared with the experimental concentrations as a function of reaction temperature.

The data shown for the first test have been derived on the fresh wash-coated monolith. A second hydrogenation test on the catalyst was performed as well, as indicated as 2nd test in Fig. 4. From Fig. 4 it is seen that CO_2 and CH_4 concentrations almost reach thermodynamic equilibrium at a reaction temperature of 240 °C in both tests. Other by-products such as CO or light hydrocarbons were not detected in either test. This test simply indicates the feasibility of wash-coating a monolith. By depositing the catalyst on a heat exchanger and removing the heat, the system can be operated at a higher temperature allowing the GHSV to be increased.

3.3. *Impact of temperature on metal dispersion in Ru/γ-Al_2O_3*

CO chemisorption was performed on the catalyst reduced at various temperatures in the range 250–550 °C to determine the effect of temperature on Ru metal dispersion. Table 1 displays Ru dispersion data for various pre-reduction temperatures. It can be seen that metal dispersion reaches its highest value of 19.24% at a reduction temperature of 320 °C. The observed increase in dispersion (from 8.37 to 19.24%) as pre-reduction temperature was increased from 250 to 320 °C suggests that Ru-containing compounds were not fully reduced to Ru^0 metal at 250 °C.

Table 1
Metal dispersion for Ru/γ-Al_2O_3 samples following reduction at different temperatures.

Reduction temperature (°C)	Ru dispersion (%)
250	8.37
320	19.24
350	11.54
550	6.93

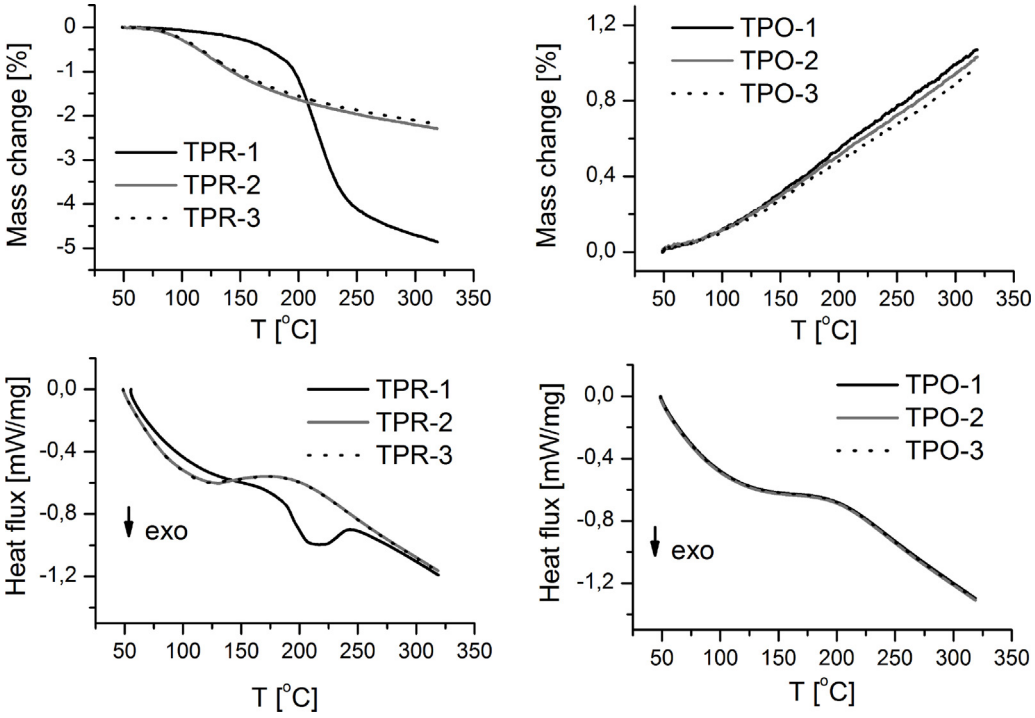

Fig. 5. TGA response for temperature-programmed reduction (top, left) and re-oxidation (top, right) and DSC signals for temperature-programmed reduction (bottom, left) and subsequent re-oxidation (bottom, right) cycles.

A significant drop in dispersion is observed at pre-reduction temperatures exceeding 320 °C. This is attributed to metal sintering. Sintering is first observed for a catalyst pre-reduced at 350 °C, when the dispersion drops to 11.54%. For a pre-reduction temperature of 550 °C, the metal dispersion is 6.93%. This demonstrates the sensitivity of the Ru/γ-Al_2O_3 catalyst to temperature and identifies metal sintering as a mode of catalyst deactivation for a reactor with poor temperature control; the use of a catalytically coated heat exchanger for CO_2 hydrogenation will eliminate this problem, provided the operating temperature is below 350 °C

3.4. Cyclic studies over Ru/Al_2O_3 followed by TGA-DSC

3.4.1. Cyclic TPO/TPR studies

The fresh Ru/γ-Al_2O_3 sample has been exposed to temperature programmed reduction and temperature programmed oxidation cycles, consecutively. The goal of this study was to further investigate the sintering and redox properties of the catalyst. It is expected that sintering in general is accompanied by a loss of oxidation and reduction behavior. Since hydrogenation is operating under reducing rather than under oxidizing conditions, the catalyst was first reduced and then re-oxidized. In Fig. 5, the response of the TGA and DSC signal occurring upon reduction and subsequent re-oxidation are compared for three TPR/TPO cycles.

As can be seen in Fig. 5, in the first applied temperature-programmed reduction cycle (TPR-1) almost no change of the mass is observed until 150 °C. A rapid decline of the mass (~5% mass loss) is seen at $T > 150$ °C. Simultaneously, the corresponding DSC function shows a minimum at $T \approx 200$ °C indicating that the rapid mass change occurs due to an exothermic reaction. Re-oxidation in O_2/N_2 (TPO-1) results in 1.2% mass increase which does not recover the mass lost during TPR-1. Hence the mass loss starting at 150 °C and the DSC function with minimum at 200 °C during TPR-1 are assigned to the decomposition of Ru-nitrate precursors in the catalyst sample which have not been fully decomposed during calcination. Calcination was deliberately performed at 250 °C to avoid forming RuO_x compounds. While this temperature is low enough to prevent the formation of volatile RuO_x species, it has likely not caused complete decomposition of the precursor salts. Note that also CO chemisorption studies as a function of pre-reduction temperature have shown that the metal dispersion is lower when the catalyst is reduced at 250 °C but increases as soon as the reduction temperature is 320 °C, also indicating that in the first TPR cycle mass loss and exothermic signal originates from decomposition of Ru-nitrate traces.

The second and third applied TPR/TPO cycles show almost identical TGA and DSC responses, indicative that after the initial H_2 treatment almost the same amount of Ru sites can be reduced and re-oxidized reversibly. Hence, significant sintering of Ru/γ-Al_2O_3 in an oxidizing and reducing atmosphere up to 350 °C is mostly excluded.

3.4.2. Isothermal cyclic studies using CO_2 and H_2 (cyclic hydrogenation)

To obtain further information about the CO_2 hydrogenation stability of the Ru/γ-Al_2O_3 catalyst, consecutive cyclic studies using TGA-DSC have been performed isothermally. The sample was exposed first to diluted CO_2 and subsequently to diluted H_2 at 260 °C. In between these treatments the sample was purged in pure N_2. This hydrogenation cycle, consisting of three gas treatments, was repeated 20 times. The TGA and DSC response is given for each cycle in Fig. 6. In Fig. 7 the first 3 cycles of this test are plotted separately to indicate the TG and DSC signals corresponding to different stages of the hydrogenation cycles. The changes of the TGA response and DSC signal are taken as a measure for the hydrogenation activity. Note that prior to this cycle study the catalyst had been reduced in H_2 at 320 °C, to avoid mass changes during the cyclic test in the TGA that may be induced by reduction or changes of the catalyst itself. That this is indeed important has been shown by the cyclic TPO/TPR treatment, discussed previously.

As expected, CO_2 treatment (at 260 °C) causes a mass increase in the thermogram and an exothermic response in the DSC. Switching

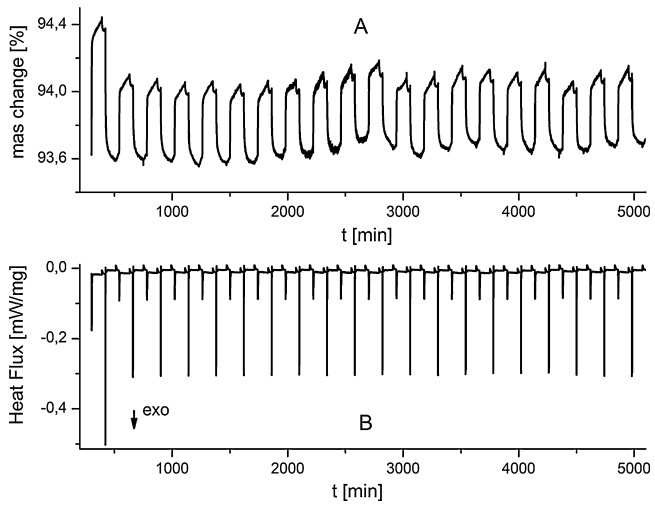

Fig. 6. TGA response (A) and DSC response (B) for consecutive introduction of first (a) CO_2/N_2, (b) N_2 and (c) H_2/N_2 at $T = 260\,^{\circ}C$. Each treatment has been applied 20 times. One cycle is defined as $CO_2/N_2 + N_2 + H_2/N_2$ introduction.

then to N_2, reduces the mass slightly by desorbing a small amount of the weakly adsorbed CO_2. Switching then to a H_2-containing stream also at 260 °C gives rise to a mass decrease and a second even more intense exothermic DSC signal. Note that the mass loss induced by H_2 introduction is essentially equal to the mass gain recorded for the CO_2 treatment. Thus, the catalyst is most likely free of any CO_2 after H_2 introduction, indicating that hydrogenation has reached full conversion under these conditions. Interestingly, only signals for the first cycle differ significantly from those obtained for the other 19 subsequent cycles. As it is seen from the mass gain and intensity of the DSC signal, the catalyst is able to chemisorb larger amounts of CO_2 in the first cycle compared to the other 19 cycles. This chemisorbed CO_2 can be fully removed by the subsequent H_2-introduction. In addition, the DSC signal induced by H_2 introduction in the first cycle is much more intense than those for the other 19 DSC signals. Conclusively, the catalyst appears to have lost sites for CO_2 chemisorption and thus lost activity. In addition, from these results it appears that the catalyst activity loss after the first cycle is of a magnitude of 40%.

However, the catalytic performance is constant for the following 19 cycles, since the area of the exothermic CO_2 and H_2 signals are almost identical. This is also the case for the mass loss and mass gain in each thermogram although a baseline drift contributes to the TGA. Since less CO_2 is adsorbed in the second cycle, it seems reasonable, to assume that active sites for CO_2 adsorption/chemisorption are irreversibly lost after the first hydrogenation cycle. Since addition of H_2 in the first cycle recovers the initial catalyst mass, it is unlikely that CO_2, or CO stays on the catalyst surface, reducing CO_2 uptake in the subsequent cycle. It is possible that elemental carbon remains on the surface, causing masking of active sites. However, if significant carbon deposition occurs in the first cycle, it would be expected that the carbon would build up over the catalyst, causing further drop in CO_2 uptake in every cycle. Sintering of Ru-sites seems to be unlikely, since the reaction temperature is only 260 °C and the catalyst has been reduced in H_2 at 320 °C for 1 h prior the first cycle. It might also be possible that Ru-sites may migrate partially into the bulk, thus lowering the number of active sites for CO_2 chemisorption. However, TPO/TPR cycle studies suggest that the catalyst can be fully re-oxidized in O_2-containing feed following prior reduction; hence a movement of Ru sites into the bulk appears to be unlikely as well. Partial re-oxidation of Ru^0 sites might be another explanation, assuming that Ru^0 sites are indispensable for CO_2 chemisorption and hydrogenation activity, respectively. Hydrogenation is assumed to be initiated by dissociation of CO_2 and subsequent CO splitting (Eqs. (4) and (5)), which is a source of oxygen atoms. Shalabi et al. have investigated the impact of H_2-pretreatment on the catalytic performance of Ni/γ-Al_2O_3 catalysts in CO hydrogenation and found that reduction in H_2 as a function of temperature and duration increases CO hydrogenation activity, suggesting indeed that Ni^0 and most likely Ru^0 is needed for high CO_2 methanation activity [40]. It should be noted

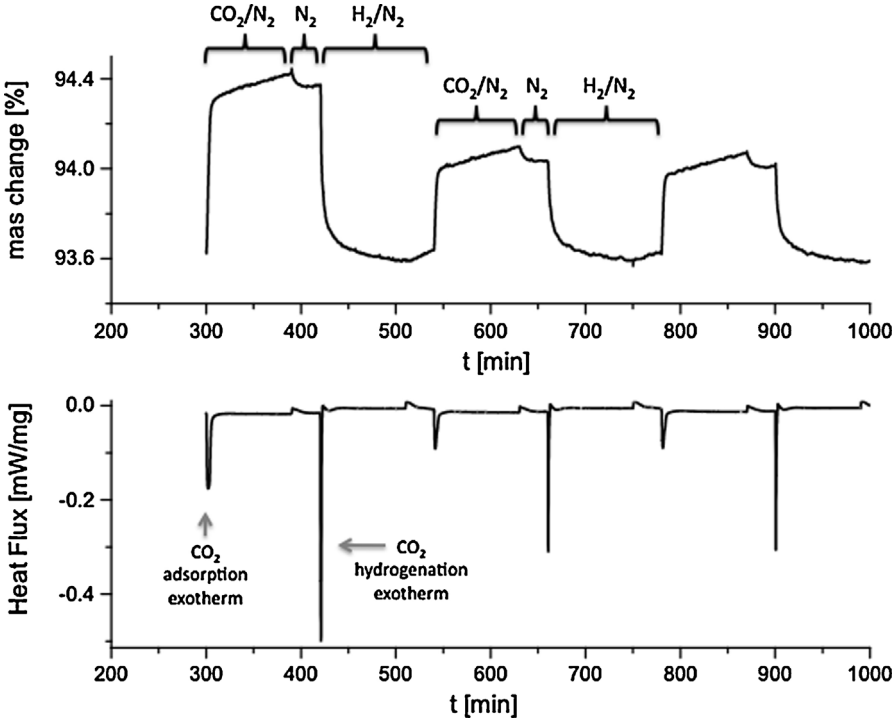

Fig. 7. TGA and DSC responses for the first 3 cycles of hydrogenation for the 20-cycle TGA-DSC test. $CO_2/N_2 + N_2 + H_2/N_2$ introduction constitute a single cycle of hydrogenation.

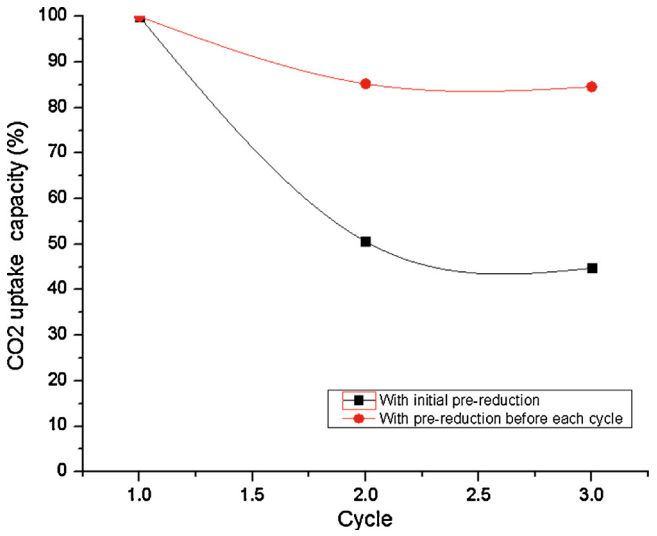

Fig. 8. Impact of H_2/N_2 treatment at 320 °C on percentage CO_2 uptake capacity at 260 °C over Ru/γ-Al_2O_3, CO_2 uptake capacity has been calculated by assigning 100% capacity to the weight gain during CO_2 introduction in the first cycle and expressing the weight gain during subsequent cycles as a percentage of this initial capacity.

that some publications suggest an alternative mechanism in which the adsorbed CO intermediate reacts directly with adsorbed hydrogen to form CH_4 [38,39]. In our TGA/DTA work, O atom production through dissociation of CO (Eqs. (4) and (5)) at 260 °C was assumed to be responsible for oxidation of Ru sites because the observed 40% decrease in active sites (in the 2nd cycle) by adsorbed CO would have produced a noticeable mass gain relative to the original catalyst weight. Furthermore our parametric studies show that CO_2 is hydrogenated to methane at 260 °C while the dispersion of Ru (and its activity) is maximized only at 320 °C. This led us to tentatively believe that some adsorbed species, possibly O···Ru, had to be removed to completely reduce the Ru to the metallic state and regain essentially all of the activity. The catalyst was treated in H_2 at 320 °C in-between each hydrogenation cycle to investigate whether re-oxidation of reduced Ru in the first cycle is responsible for the decline in CO_2 chemisorption and hydrogenation activity. Results are shown in the next section.

3.4.3. *Isothermal cyclic studies using CO_2 and H_2 with pre-treatment by reduction at 320 °C*

Three isothermal hydrogenation cycles (including CO_2, N_2, and H_2 treatment at 260 °C) have been performed with and without inter-cycle H_2-treatment at 320 °C. It was assumed that the loss in CO_2 chemisorption and hydrogenation activity due to re-oxidation of Ru-sites after the first cycle can be suppressed by reducing the catalyst in-between each hydrogenation cycle.

In Fig. 8 the CO_2 uptake capacity is shown with and without inter-cycle H_2-treatment. As evident, the regeneration with added H_2 in between each cycle improves the CO_2 uptake capacity (top curve) relative the uptake in the absence of the H_2 treatment (bottom curve). A higher CO_2 uptake capacity for the second and third cycle is seen when the catalyst was treated with H_2 at 320 °C between each cycle. Recovery of 90% of initial CO_2 uptake capacity upon H_2-treatment shows that the catalyst does not undergo significant irreversible deactivation during CO_2 hydrogenation at 260 °C. Although further testing is needed to confirm the link between Ru^0 oxidation and loss of CO_2 chemisorption sites, these results are supportive of our hypothesis that the loss of CO_2 uptake after the first cycle is likely due to re-oxidation of Ru^0 by the O atoms produced during the dissociation of CO_2.

4. Conclusions

The CO_2 methanation at 1 bar and $H_2/CO_2 = 4$ has been investigated over a 10% Ru/γ-Al_2O_3 catalyst in terms of the process parameters, thermal and cyclic stability. At low space-velocity of 4720 h^{-1} thermodynamic equilibrium was essentially reached at $T \approx 280$ °C. At high space-velocity and high operating temperatures traces of CO were detected, suggesting that the rate of RWGS is higher than that of CO hydrogenation. The catalyst showed no sign of deactivation for 8 start-up/shut-down cycles and for total time on stream of 72 h, respectively. In addition, cyclic TGA-DSC studies in CO_2 and H_2, being introduced consecutively at 260 °C, suggest a high stability of the Ru-catalyst, although it was found that CO_2 chemisorption and hydrogenation activity was lowered by a magnitude of 40% after the first cycle. However, the catalyst showed stable activity for the following 19 cycles. A H_2 treatment between each cycle at 320 °C can prevent the apparent loss in activity. It is proposed that the decrease in CO_2 hydrogenation activity after the first cycle is due to partial re-oxidation of Ru^0 sites, which occurs due to the dissociation of CO_2 and/or CO to C and O. The H_2 treatment reduces those Ru···O sites converting them to active Ru metal sites. Supportively, a cyclic TPO/TPR study followed by TGA/DSC on Ru/γ-Al_2O_3 suggests that the catalysts can be indeed re-oxidized almost fully in an oxidizing feed.

A 10% Ru/γ-Al_2O_3//monolith has been investigated catalytically as well. Excellent selectivity to methane and CO_2 conversions under low space-velocity conditions were achieved at low hydrogenation temperatures. Thus, we propose that Ru/γ-Al_2O_3 is a suitable candidate for being wash-coated on a heat exchanger to remove the heat liberated. This provides a pathway to a new reactor design utilizing washcoated heat exchangers as opposed to many particulate beds in tubular reactors surrounded by a cooling medium.

Acknowledgement

Financial support from BASF is gratefully acknowledged.

References

[1] G. Centi, S. Perathoner, Greenhouse Gases: Science and Technology 1 (2011) 21–35.
[2] J.H. McCrary, G.E. McCrary, T.A. Chubb, J.J. Nemecek, D.E. Simmons, Sol. Energy 29 (1982) 141–151.
[3] D.R. Lutz, Reliable Carbon-neutral Power Generation System, USA, 2008.
[4] K. Hashimoto, M. Yamasaki, K. Fujimura, T. Matsui, K. Izumiya, M. Komori, A.A. El-Moneim, E. Akiyama, H. Habazaki, N. Kumagai, A. Kawashima, K. Asami, Mater. Sci. Eng. A 267 (1999) 200–206.
[5] R.J. Farrauto, Y. Liu, W. Ruettinger, O. Ilinich, L. Shore, T. Giroux, Catal. Rev. 49 (2007) 141–196.
[6] D.C.D. da Silva, S. Letichevsky, L.E.P. Borges, L.G. Appel, Int. J. Hydrogen Energy 37 (2012) 8923–8928.
[7] T. Van Herwijnen, H. Van Doesburg, W.A. De Jong, J. Catal. 28 (1973) 391–402.
[8] P.J. Lunde, F.L. Kester, Ind. Eng. Chem. Proc. Des. Dev. 13 (1974) 27–33.
[9] A. Karelovic, P. Ruiz, J. Catal. 301 (2013) 141–153.
[10] A. Karelovic, P. Ruiz, Appl. Catal. B: Environ. 113-114 (2012) 237–249.
[11] C. Deleitenburg, A. Trovarelli, J. Catal. 156 (1995) 171–174.
[12] J.-N. Park, E.W. McFarland, J. Catal. 266 (2009) 92–97.
[13] C. Schild, A. Wokaun, A. Baiker, J. Mol. Catal. 69 (1991) 347–357.
[14] A. Erdöhelyi, M. Pásztor, F. Solymosi, J. Catal. 98 (1986) 166–177.
[15] S. Hwang, U.G. Hong, J. Lee, J.G. Seo, J.H. Baik, D.J. Koh, H. Lim, I.K. Song, J. Ind. Eng. Chem. (2013).
[16] G. Zhou, T. Wu, H. Xie, X. Zheng, Int. J. Hydrogen Energy (2013).
[17] N. Srisawad, W. Chaitree, O. Mekasuwandumrong, A. Shotipruk, B. Jongsomjit, J. Panpranot, React. Kinet. Mech. Cat. 107 (2012) 179–188.
[18] A.E. Aksoylu, A.N. Akin, Z.İ. Önsan, D.L. Trimm, Appl. Catal. A: Gen. 145 (1996) 185–193.
[19] J.L. Falconer, A.E. Zağli, J. Catal. 62 (1980) 280–285.
[20] M. Cai, J. Wen, W. Chu, X. Cheng, Z. Li, J. Nat. Gas Chem. 20 (2011) 318–324.
[21] S. Sharma, Z. Hu, P. Zhang, E.W. McFarland, H. Metiu, J. Catal. 278 (2011) 297–309.
[22] H. Song, J. Yang, J. Zhao, L. Chou, Chinese J. Catal. 31 (2010) 21–23.
[23] N. Takezawa, H. Terunuma, M. Shimokawabe, H. Kobayashib, Appl. Catal. 23 (1986) 291–298.
[24] R. Spinicci, A. Tofanari, Appl. Catal. 41 (1988) 241–252.

[25] F.-W. Chang, M.-T. Tsay, S.-P. Liang, Appl. Catal. A: Gen. 209 (2001) 217–227.
[26] A. Borgschulte, N. Gallandat, B. Probst, R. Suter, E. Callini, D. Ferri, Y. Arroyo, R. Erni, H. Geerlings, A. Zuttel, Phys. Chem. Chem. Phys. 15 (2013) 9620–9625.
[27] T.K. Campbell, J.L. Falconer, Appl. Catal. 50 (1989) 189–197.
[28] H. Liu, X. Zou, X. Wang, X. Lu, W. Ding, J. Nat. Gas Chem. 21 (2012) 703–707.
[29] Z.L. Zhang, A. Kladi, X.E. Verykios, J. Catal. 148 (1994) 737–747.
[30] Z. Kowalczyk, K. Stołecki, W. Raróg-Pilecka, E. Miśkiewicz, E. Wilczkowska, Z. Karpiński, Appl. Catal. A: Gen. 342 (2008) 35–39.
[31] M. Schoder, U. Armbruster, A. Martin, Chem. Ing. Tech. 85 (2013) 344–352.
[32] C.K. Vance, C.H. Bartholomew, Appl. Catal. 7 (1983) 169–177.
[33] C. Galletti, S. Specchia, G. Saracco, V. Specchia, Chem. Eng. Sci. 65 (2010) 590–596.
[34] P. Panagiotopoulou, D.I. Kondarides, X.E. Verykios, Appl. Catal. B: Environ. 88 (2009) 470–478.
[35] P. Panagiotopoulou, D.I. Kondarides, X.E. Verykios, Appl. Catal. A: Gen. 344 (2008) 45–54.
[36] F. Solymosi, A. Erdohelyi, M. Kocsis, J. Chem. Soc. Faraday Trans. 1 77 (1981).
[37] E. Zagli, J.L. Falconer, J. Catal. 69 (1981) 1–8.
[38] M. Marwood, R. Doepper, A. Renken, Appl. Catal. A: Gen. 151 (1997) 223–246.
[39] P. Panagiotopoulou, D.I. Kondarides, X.E. Verykios, J. Phys. Chem. 115 (2011) 1220–1230.
[40] M.A. Shalabi, S.A. Zaidi, M.A. Al-Saleh, Chem. Eng. Commun. 157 (1997) 23–33.